Phage Resistance Mechanisms Increase Colistin Sensitivity in *Acinetobacter baumannii*

Xiaoqing Wang[1,2], Belinda Loh[1], Yunsong Yu[3,4], Xiaoting Hua[3,4]*, and Sebastian Leptihn[5,3,1]*

[1] Zhejiang University-University of Edinburgh (ZJU-UoE) Institute, Zhejiang University, Haining, China

[2] Medical school, Lishui University, Lishui, China

[3] Department of Infectious Diseases, Sir Run Run Shaw Hospital, Zhejiang University School of Medicine, Hangzhou, China

[4] Key Laboratory of Microbial Technology and Bioinformatics of Zhejiang Province, Hangzhou, China

[5] University of Edinburgh Medical School, Biomedical Sciences, College of Medicine & Veterinary Medicine, The University of Edinburgh, Edinburgh, United Kingdom

* Correspondence can be addressed to:

Prof. Xiaoting Hua, xiaotinghua@zju.edu.cn, Sir Run Run Shaw Hospital, Hangzhou, China, East Qingchun Rd 3, Jianggan District, Hangzhou 310016, P. R. China

Prof. Sebastian Leptihn, sebastian.leptihn@ed.ac.uk, Infection Medicine, Biomedical Sciences, Edinburgh Medical School, College of Medicine and Veterinary Medicine, The University of Edinburgh, 47 Little France Crescent, EH16 4TJ Edinburgh, United Kingdom

ABSTRACT: Few emergency-use antibiotics remain for the treatment of multidrug-resistant bacterial infections. Infections with resistant bacteria are becoming increasingly common. Phage therapy has reemerged as a promising strategy to treat such infections, as microbial viruses are not affected by bacterial resistance to antimicrobial compounds. However, phage therapy is impeded by rapid emergence of phage-resistant bacteria during therapy. In this work, we studied phage-resistance of colistin sensitive and resistant *A. baumannii* strains. Using whole genome sequencing, we determined that phage resistant strains displayed mutations in genes that alter the architecture of the bacterial envelope. In contrast to previous studies where phage-escape mutants showed decreased binding of phages to the bacterial envelope, we obtained several not uninfectable isolates that allowed similar phage adsorption compared to the susceptible strain. When phage-resistant bacteria emerged in the absence of antibiotics, we observed that the colistin resistance levels often decreased, while the antibiotic resistance mechanism *per se* remained unaltered. In particular the two mutated genes that conveyed phage resistance, a putative amylovoran- biosynthesis and a lipo-oligosaccharide (LOS) biosynthesis gene, impact colistin resistance as the mutations increased sensitivity to the antibiotic.

Running title: Phage resistance in colistin resistant *A. baumannii*

Keywords: Phage; Phage Therapy; Phage-resistance; Phage Adsorption; Colistin Resistance; Antibiotic Resensitation; Virulence;

Introduction:

Antimicrobial resistance (AMR) is a global concern. The overuse of antibiotics in human medicine and the misuse of even last resort antimicrobial compounds such as colistin in agriculture, is contributing to the increasing number of antibiotic resistant bacterial pathogens (1). For most antibiotics, molecular mechanisms of resistance have evolved which are quickly distributed throughout bacterial populations by horizontal gene transfer. This is primarily mediated by plasmids and ICEs (2-4). At the same time, the slow and expensive discovery process and clinical development of antimicrobial compounds together with the lack of monetary incentives have resulted in continuously decreasing numbers of effective drugs to treat bacterial infections (5, 6).

The last resort antibiotic colistin is often accompanied by strong side effects, have to be deployed for infections by multidrug resistant pathogens. Here, colistin has gained importance for clinical use. However, colistin resistance in pathogens is increasing as well. Phage therapy has emerged as a promising strategy to treat drug resistant bacterial infections, as viruses are not affected by resistance to antimicrobial compounds (7-9). Phage therapy is the use of lytic phages that have the ability to inactivate pathogens. However, phage-resistance, i.e. the emergence of bacterial mutants that are resistant to a therapeutic phage, is commonly observed (10). Several solutions have been explored in the past, such as combinational phage-antibiotic therapeutic courses, where synergetic effects are often observed, or the deployment of phage mixtures (“phage cocktails”). Yet, in the majority of clinical trials phage-resistance occurs (11). Therefore, it is important to understand the mechanisms that enable bacteria to gain resistance to phages and the consequences of selection. In addition, identifying target molecules that facilitate phage infection and deployment of phages that do not bind the same receptors has been proposed to decrease the likelihood of phage-resistance (12).

In order to understand molecular mechanisms of phage-resistance, we investigated a phage-pathogen system consisting of the type strain of *A. baumannii* and a colistin-resistant mutant of ATCC17978. We employed whole genome sequencing of phage-escape mutants that emerged after co-incubating the novel phage Phab24 that infects both strains. We found that genes abolishing infection are primarily involved in the biogenesis of the envelope of the bacterial host, namely LPS (LOS) and capsular polysaccharides. The two genes we identified in *A. baumannii* are involved in the biosynthesis of the bacterial envelope; the putative amylovoran biosynthesis gene *amsE* is involved in capsule formation while *lpsBSP* plays a role in lipo-oligosaccharide (LOS) biosynthesis. While an *amsE* deletion leads to decreased adsorption, the mutation in the *lpsBSP* gene does not alter binding of the phage to the bacterial surface. Gene engineered strains introducing the observed mutations one at a time in the parental strain, and their complementation with the wildtype gene *in trans*, confirmed the role of the genes in phage-resistance. *In vitro* evolution experiments resulted in the selection of escape mutants with decreased antibiotic resistance, with mutations in *amsE* contributing to this effect.

Results

Isolation of Phage Phab24 that infects Colistin-Resistant *A. baumannii* Strain XH198

Colistin resistance is mediated by a fundamental change in the bacterial membrane composition. A mutation in gene *pmrB* (G315D) results in surface modification of the bacterial envelope, preventing efficient colistin binding and thus mediating resistance to the antibiotic (13-17). To study phage-resistance of bacteria *in vitro,* we used the colistin resistant *Acinetobacter baumannii* strain XH198 and its non-resistant parental strain ATCC17978. Strain XH198 was obtained by an *in vitro* evolution experiment and exhibits altered LOS molecules, which has also been observed in clinical isolates, rendering colistin ineffective (14). We isolated several phages that are able to infect both, XH198 and ATCC17978. To focus on one particular virus-host system, we selected a phage that we named Phab24, for Phage *Acinetobacter baumannii* number 24 (genome accession number: MZ477002) (Figure 1A). Whole genome analysis using the programme PhageAI (https://phage.ai/) revealed that bacteriophage Phab24 is virulent (lytic) with a 93.76% confidence in prediction (18).

Isolation and characterisation of phage-resistant bacterial mutants:

We first used the phage-host system of Phab24 and ATCC17978, to study the emergence of phage-resistant bacterial mutants, by co-incubating both in liquid media. Subsequently, bacteria were plated on solid media from which we randomly picked 80 bacterial colonies (R1-R80). Surprisingly, two isolates displayed susceptibility to Phab24, possibly persister cells (19) while the remaining 78 were resistant to Phab24. Similarly, from co-incubating Phab24 with XH198, the colistin-resistant derivative of the ATCC reference strain, we isolated 400 colonies at random. Next, we sequenced the whole genome of six of the phage-resistant isolates of ATCC17978 (R5, R10, R22, R23, R39, R70) and nine of

XH198 (R81, R83, R86, R115, R125, R130, R132, R134, R137). Using Breseq (20), we found several point mutations as well as deletions or insertions in genes that might mediate phage-resistance, which were confirmed by PCR and subsequent sequencing (Table 1 and Supplemental table 1). The most common gene to have mutations codes for a putative LPS biosynthesis protein, which we subsequently called *lpsBSP* (gene AUO97_03485). Here, we observed a single nucleotide deletion or an IS insertion, indicating parallel emergence of phage resistance. We also found mutations in genes predicted to code for glycosyltransferases (glycosyl transferase 1, AUO97_06920 and glycosyl transferase 2 AUO97_03485), phosphohydrolase *phoH* and the putative ABC transporter *abcT*. While we found many mutations in genes that were later identified to be irrelevant for phage-resistance, we also identified two types of mutations (a frameshift or an insertion) in a gene called *amsE* (AUO97_06900), which encodes a putative amylovoran biosynthesis protein.

To demonstrate that the mutations indeed render a strain non-susceptible, we constructed several plasmids encoding the wildtype genes in the *A. baumannii* shuttle vector pYMAb2 (21, 22). We then introduced the episomal elements into the phage-resistant (R) -mutants. The expression of the wildtype genes of the LPS biosynthesis protein *lpsBSP* (e.g. in R1) as well as of *amsE* (e.g. in R7) did restore phage sensitivity, unless they were both present in the strain (e.g. strain R5) (Table 1). Some phage-resistant isolates could not be complemented by wildtype genes coding for some of the mutations we observed (e.g. the membrane transport protein *abcT, phoH,* or *actP*), indicating the presence of additional, as of yet unidentified, mutations that confer resistance (Supplemental table 1).

Due to the obvious complexity of the resistance mechanisms, we decided to focus on *lpsBSP* and *amsE*. To demonstrate the role of these genes in phage susceptibility, in addition to complementations *in trans*, we engineered the mutations into the parental *A. baumannii* strain (ATCC17978), or created knock-out mutants of genes. When mutations

are introduced into the gene coding for *lpsBSP*, the bacterium is rendered "immune" to phage Phab24 (Figure 1B). Similarly, a reconstructed mutant in which the *amsE* gene is deleted cannot be infected by the phage, clearly demonstrating the role of these two genes in phage susceptibility. Both reconstructed mutants can be infected by Phab24, when the complementing wildtype genes are expressed *in trans*, from plasmids (Figure 1A and B).

Attachment of Phab24 to the surface of phage-resistant mutants

As the mutations found in *lpsBSP* and *amsE* code for putative proteins involved in LOS and capsule formation, respectively, we concluded that the surface of the phage-resistant mutants may exhibit modifications compared to the wildtype. Changes on the surface of mutant strains might therefore lead to a reduction in binding of phages to bacteria. We therefore performed binding assays to assess the quantity of phages that bind to the bacterial envelope. To this end, we co-incubated Phab24 with the phage-resistant mutants and controls for 20 minutes and subsequently determined the phage titre left in the supernatant (Figure 2). The positive control, strain ATCC17978, was able to reduce the titre by a factor of more than 1000-fold, while the negative controls (no bacteria or *A. baumannii* strain XH194 resistant to Phab24 infection) resulted only in a minor reduction in the number of phage particles in the supernatant. Interestingly, Phab24 bound ATCC17978 with an apparent binding affinity higher than XH198. The *amsE* knockout on the backbone of ATCC17978 showed reduced bacteriophage binding, similar to the negative controls. However, upon complementation with the wildtype *amsE* gene *in trans*, binding of Phab24 was restored to a level comparable to parental ATCC17978. However, the *lpsBSP* knockout and its derivative complemented with wildtype *lpsBSP* both bound Phab24 avidly just like the parental ATCC17978 strain. Surprisingly, with the exception of *amsE* mutants, phage Phab24 still binds to most phage-resistant strains (Figure 2B).

The bacterial envelope is altered in both, the LPS biosynthesis protein mutant and the *amsE* mutant

LPS often serves as a co-receptor in phage binding. As a disruption in the gene coding for a LPS biosynthesis protein (*lpsBSP*) was observed, we determined if the mutations in the isolated strains lead to a change in LPS composition. Mass spectrometry of isolated lipid A, obtained using the hot aqueous phenol extraction method, was performed to compare the reconstructed mutants (on the ATCC17978 backbone) with the ATCC17978 control (Figure 3A and B). In addition, we analysed the samples of the plasmid-complemented strain that allows the expression of *lpsBSP in trans*. Previously, it was established that the m/z of *A. baumannii* lipid A is featured as a prominent peak at 1,910, which was identified as a singly deprotonated lipid A structure that contains two phosphate groups and seven acyl chains (i.e., diphosphoryl hepta-acylated lipid A) (23). In our experiments, this peak was observed in all samples (Figure 3). While the mass spectrum of the KO strain (Figure 3B) shows molecules with mass / charge (m/z) values of 1,910 and smaller, the reference spectrum (Figure 3A) exhibits several additional small peaks larger than 2,000. These higher molecular weight peaks are more prominent in the plasmid-complemented strain (Figure 3C). While the identification of molecules that lead to the occurrence of these peaks with higher m/z values is still outstanding, they possibly represent modified Lipid A molecules. As these peaks are indistinguishable from the baseline spectrum recorded with the KO strain sample (Figure 3B), it may be reasonable to conclude that the disruption in *lpsBSP* results in a modification in the bacterial surface structure. The gene disruption might ultimately prevent the incorporation of one or more types of modified LPS molecules into the bacterial envelope which are able to facilitate specific Phab24 phage binding (15, 23).

As *amsE* is a putative amylovoran biosynthesis protein involved in the production of amylovoran, an acidic exopolysaccharide (EPS), we isolated the oligosaccharides of the reconstructed *amsE* mutant and to compare strain ATCC17978, and again performed mass spectrometry without the intension to characterise the molecules observed in the spectra. We only used the method to compare the mass spectrometry results to each other. Perhaps unexpectedly, we did not observe any additional presence or absence of peaks in the spectra across 180-3200 m/z (Supplemental Fig. 1, 2, 3). While ratio and intensity varied for some peaks, there is no indication of the absence of specific polysaccharides, or the presence of others, in the *amsE* mutant. The relative quantity of the polysaccharides cannot be firmly established with the method we employed, and thus we attempted to determine if differences can be seen on SDS PAGE gels which allow a separation of molecules based on size, while also allowing a quantitative analysis. Here, we observed that the genetically engineered *amsE* mutants of ATCC17978 or of XH198 exhibited a massive reduction in material on the gel compared to the complemented strains (and the reference strains) where *amsE* was expressed *in trans* (Figure 3D, E). A gel with Alcian blue, which stains acidic polysaccharides, shows that the *amsE* mutants of both, ATCC17978 and XH198, contain almost undetectable amounts of material, while the plasmid-complemented strains are similar to the wildtype level. In addition to large molecular weight bands, we also observe small molecule components which are stained by Alcian blue, but also by silver ions. As silver staining allows the sensitive detection of lipids and proteins but not of the saccharides (and polypeptides can be excluded due to the preparation which includes a Proteinase K digestion step), the smaller molecules possibly indicate the presence of lipid-saccharide conjugates in the samples, which again, are absent in the *amsE* mutants. Although the mass spectrometry data did not indicate any changes in saccharide composition, the quantitative method of size-separated oligosaccharides on gels indicate that the bacterial envelope surface (possibly not the

217 composition) of the *amsE* mutant is clearly different from that of the *A. baumannii*
218 reference strain.

219 **Changes in cell morphology and capsule formation in phage-escape mutants.**

220 On the molecular level we could confirm that the composition of the cell envelope is
221 different in the *lpsBSP* mutant while we found no indication for a qualitative change in the
222 *amsE* mutant, although the mutant appears to produce substantially less
223 exopolysaccharides. However, it is difficult to conclude that the surface structure of the
224 cells is altered by the mutations. We first employed Transmission electron microscopy on
225 thin sections of resin-embedded cells with inconclusive results (Supplemental Figure 2).
226 We then used Scanning Electron Microscopy where, both, ATCC17978 and XH198 cells,
227 appear similarly smooth and rod-shaped. A similar morphology could be observed in the
228 case of cells containing the *lpsBSP* mutant; when complemented *in trans* by the functional
229 gene, a slightly more “shrivelled” -possibly desiccated- structure was observed. A very
230 even, smooth surface was seen when the *amsE* mutant was complemented with the
231 functional gene *in trans* while the surface of the *amsE* mutant itself appeared less smooth.
232 In addition, the cells of the *amsE* mutant appear more rounded and adherent to each
233 other, forming clusters (Figure 4). We also observed the formation of mucoid-like strings in
234 preparations of the *amsE* mutant which were absent in all other samples (Supplemental
235 Figure 3).

236 The observed clustering and appearance of “slime” on the surface of the *amsE* mutant
237 may be caused by exopolysaccharide and/or biofilm formation. We therefore assessed the
238 production of material produced by cells grown for three days to retain the dye crystal
239 violet, often used to quantify the extent of biofilm produced by bacteria. Here, we observed
240 that biofilm formation (the ability to retain the dye) was most pronounced in the colistin
241 resistant strain XH198, but remained low in all other strains (Figure 5). Compared to the
242 reference strain ATCC17978, the *amsE* mutant showed reduced biofilm formation (~42 %

reduction compared to ATCC17978), while plasmid complementation led to a slight increase in biofilm (~117% of that of ATCC17978) (Figure 5A). In the case of the *lpsBSP* mutant, no significant difference in biofilm formation of the complemented or non-complemented strains was observed. Thus, the "mucoid" appearance and aggregation observed in SEM preparations of the cells in the *amsE* mutant cannot be explained by the formation of biofilms. Interestingly, we observed the formation of highly fragile membraneous structures in the multi-well plates for this mutant that, however, did not retain the dye, and were washed away easily (Supplemental Figure 4). In addition to the formation of biofilms we also employed crystal violet staining of capsules of planktonic cells. Biofilms are usually formed if bacteria are incubated for a long duration and allowed to sediment and form clusters. If cells are incubated for shorter times under shaking, biofilm formation does not occur. It is reasonable to assume that the amount of dye that is retained by the capsule correlates with the quantity material present for the dye to embed in (i.e. more dye is retained by more extensive capsules) and/ or the density of the packing of the capsule material (i.e. released quicker if the material is less compact). The ATCC17978 strain retained substantially more dye compared to the *amsE* mutant while a complementation results in the same levels observed for the reference strain (Figure 5B). One interpretation is that the *amsE* mutant strain can absorb less dye due to a smaller capsule which would correlate with the results of the capsular material separated on SDS gels (Figure 3). The *lpsBSP* mutant exhibits slightly more absorption of the dye, while the complemented strain shows levels identical to ATCC17978.

AmsE and LPS biosynthesis mutants are less virulent *in vivo*

As part of the extended bacterial surface structure, to which capsules can be included, LPS/LOS and capsular molecules often contribute to virulence of strains (24-27). We therefore investigated how the genes that conferred phage-resistance impact the virulence

of the phage-escape mutants. To this end, we used the insect larva model *Galleria melonella*, to assess the virulence of the reference strains (ATCC17978, XH198), compared to the single gene mutant strains (*amsE*, *lpsBSP*), and those complemented *in trans*. The mutation in *lpsBSP* impacts the virulence of the strain only to a small extent, with slightly increased survival rates compared to ATCC17978 (Figure 6). In contrast, the *amsE* KO strain had a significantly reduced virulence, demonstrating the importance of *amsE* on the pathogenicity of *A. baumannii*. When the *amsE* mutant strain was complemented with a plasmid expressing the wildtype gene under a constitutive promotor, the virulence was significantly increased compared to ATCC17978, possibly due to a higher expression level. Similarly, albeit to a lesser extent, virulence of the strain with the *lpsBSP* mutation increased when the wildtype gene was expressed *in trans*.

Phage-resistance mutations in *amsE* decrease colistin resistance:

Specific alterations in membrane composition are the molecular basis for colistin resistance. We found that phage Phab24 binds to surface exposed molecules of ATCC17978 and XH198, and resistance is mediated by altered envelope structures. To answer the question if the resistance mechanisms have impact on each other, we performed experiments testing the combination of Phab24 together with colistin. During phage therapy, antibiotics are often used in combination with therapeutic phages, as synergistic effects of phage-antibiotic combinations have often been observed (28, 29). In our case, increasing concentrations of phage reduced the apparent MIC of colistin (Figure 7A). One explanation is that phage-resistant mutants show a higher sensitivity to colistin. To address this hypothesis, we investigated if phage-resistant bacteria show higher sensitivity to colistin, testing colony survival of XH198 cultures grown in the absence of colistin but with Phab24 (MOI of 1) (Figure 7B and C). The numbers of colony forming units (CFUs) were subsequently determined on media with different amounts of colistin.

Interestingly, we observed that the number of CFU decreases with increasing colistin concentration, regardless whether or not the bacteria were co-incubated with Phab24. Compared to the number of colonies that grew on plates without colistin, the ratio of bacterial colonies dropped by ~1/4 to ~3/4 when colistin was present. However, in the presence of Phab24, the ratio of CFUs was reduced to less than 0.01% compared to the count when colistin was absent. This observation might indicate that the selection for phage-resistance leads to the mutations which in turn increase the sensitivity to colistin.

To investigate this finding in more detail, we tested the MIC of individual phage-resistant XH198 mutants (Figure 7D). Resistance levels varied widely from 64 to 0.5 mg/L (Supplemental Table 2). The correlation between the observed reduction in colistin resistance with phage resistance is far from trivial. Colistin resistance in the parental strain XH198 is mediated by a mutation in gene *pmrB* (G315D), which remained unchanged (data not shown). Therefore, the molecular basis for increased sensitivity possibly lies in other mutations found in the strains, including those in *amsE* or *lpsBSP*. Thus, we tested the impact of *amsE* and *lpsBSP* on the colistin sensitivity.

We first tested XH198-derived phage resistant isolates with *lpsBSP* mutations, R518 and R587, where we observed a colistin MIC of 2 mg/ L. Both strains can be complemented with a plasmid-encoded *lspBSP* which then allows infection by Phab24 increasing the MIC to 64 mg/ L (Figure 7D). While the strains may have additional mutations, this might be an indication that the *lpsBSP* mutation increases colistin sensitivity. Curiously, the genetic deletion of the entire *lpsBSP* gene in XH198 (a knock-out) appears does not result in a reduction in colistin resistance. We then tested the reconstructed *amsE* mutant on the backbone of XH198, which showed strongly increased sensitivity to colistin, from 64 mg/ L to 8 mg/ L (Figure 7D). The complementation *in trans* using a plasmid-encoded wildtype *amsE* restored the high resistance level to colistin. Similarly, mutants containing *amsE* mutations exhibiting various degrees of colistin sensitivity, displayed the high level of

resistance when complemented e.g. R130 from 4 mg/ L (without plasmid), to 64 mg/ L (with plasmid).

Discussion

Bacterial phage susceptibility rests on several mechanisms, one of which is binding to receptors and co-receptors. In our work, we have established the role of two genes in permitting the infection of *A. baumannii* strain ATCC17978 and its colistin-resistant derivative, XH198 by phage Phab24. We provide evidence that the genes encode proteins that are involved in the biogenesis of the bacterial envelope and function as phage receptors (or receptor and co-receptor). One gene has a putative function in the biogenesis of LPS (or LOS), which we named *lpsBSP*. The second gene, *amsE*, is likely involved in the biosynthesis of amylovoran for capsular exopolysaccharide production.

Previous work has shown that capsular molecules can serve as phage receptors, which we also show describe in this study (30-33). Phage-resistant isolates that displayed mutations in *amsE* did not permit efficient binding or infection by Phab24. These mutations may either lead to the production of altered surface receptors to which the phage cannot bind, or perhaps abolish the production of the "correct" receptor. Surprisingly, we found that binding is unaltered in strains displaying mutations in *lpsBSP*, yet infection does not occur, which contrasts with previous reports (34, 35). For some phages, the simultaneous binding of receptor and co-receptor is essential for the release of DNA into the host. For Phab24, we believe that a specific type of LOS molecule, which is not present in the mutant strain, is required to trigger the release of DNA into the bacterium, while the phage is able to bind via capsular polysaccharides in whose production *amsE* is involved.

The work presented here points to phage resistance being caused by an alteration of the bacterial surface structure. Phage resistance caused by capsule loss has been described previously and the same publication also reports that a phage-escape mutant of a *A.*

347 *baumannii* MDR strain showed a much reduced propensity to form biofilms (34). In our
348 work, we also observed a decrease in the formation of biofilm when investigating the *amsE*
349 gene knockout in the colistin sensitive reference strain ATCC17978.
350 Our study also showed that the two mutations that conferred phage-resistance result in
351 decreased virulence in our *in vivo* model. Similar to our findings, it has been shown that
352 phage escape mutants often show attenuated pathogenicity which, in some instances, is
353 thought to be due to bacterial envelope modifications which are the basis of phage
354 resistance (34, 36-39). Increasing evidence indicates that phage-resistance is a “trade-off”
355 that results in decreased virulence and increased susceptibility to antibiotics (40).
356 Therapeutic bacteriophages are commonly deployed together with antibiotics in clinical
357 therapy. This is often done despite the fact that the bacteria display antibiotic resistance to
358 the used compounds *in vitro*, due to the often observed phage-antibiotic synergy which we
359 have also observed here (11, 28, 41-43). In our work, we saw a decrease in apparent MIC
360 when colistin was used in combination with phage Phab24. The emerging phage-resistant
361 bacterial clones often exhibited increased levels of antibiotic sensitivity. Previously, it has
362 been proposed that phages could be used to re-sensitise bacterial pathogens to antibiotics
363 (34, 44, 45). When we attempted to elucidate the underlying mechanisms, we found that
364 phage resistant mutants with disruptions in *amsE* resulted in a drastic increase in colistin
365 sensitivity, while the original mechanism for colistin resistance remained unaffected.
366

367 **Acknowledgements**

368 We thank Mark Toleman (University of Cardiff) for critically reading the manuscript, to Nick
369 Scott (University of Melbourne) for helpful discussions. We thank Belinda Loh who has
370 obtained no financial compensation nor salary from the affiliated institution for her work
371 during the last year.
372

373 SL, XH, YY and BL contributed to study conception and design. XW performed the
374 experiments. XW, SL, BL analysed the data. SL supervised the study. SL and BL wrote
375 the manuscript. All authors approved the final manuscript.
376

Materials & Methods

Isolation, purification and the genome of phage Phab24 is described elsewhere (Manuscript submitted to *Genome announcement*). Genome accession number: MZ477002.

DNA genome sequencing and analysis. Genomic DNA was extracted using Bacterial genome DNA isolation kit (Biomed, China), sequenced by Illumina HiSeq (150-bp paired reads) and assembled using Unicycler version 0.4.8 (46). Breseq was used to identify single point mutations (20).

Gene knockout or replacement and complementation were performed as described previously: (47).

Determination of bacterial growth rates was performed as described previously (48) with the following modifications for experiments that included phages: An MOI of 5 of a high-titre preparation was added to the culture with a negligible dilution.

Transmission electron microscopy was performed as described previously: (49). Micrographs were obtained with a JEOL JEM1010 at 80 kV. Scanning Electron Microscopy as described here: (21).

Phage adsorption. Adsorption was measured indirectly by quantifying free phage in solution. Overnight bacterial culture was diluted in LB and bacteria at 8×10^9/mL were incubated with Phab24 at 2×10^9/mL at 4□ for 20 minutes. Cells were pelleted by centrifugation, before the supernatant was serially diluted and non-adsorbed phages quantified by spot titre.

403

404 Laboratory evolution experiment: The soft-agar overlay technique was used to obtain
405 phage resistant colonies which are purified three times by re-streaking, after co-incubation
406 of ATCC17978 (or XH198) with Phab24 (MOI = 1) for 3 hours at 37˚C.

407

408 Colistin MIC was determined by the broth-dilution method as described previously: (14).

409

410 Lipid A isolation and structural characterisation: Lipid A isolation was performed as
411 previously described (50) which was used for MALDI-MS.

412

413 Surface polysaccharide extraction were purified by hot aqueous phenol extraction
414 according to a previously described protocol (51).

415

416 Biofilm assays were preformed as described previously: (52). Each sample was done five
417 times, with 3 independent experiments.

418

419 Crystal Violet (CV) retention assay of planktonic cells: Overnight cultures were diluted in
420 LB media to OD600 = 1. 1 mL of diluted culture was centrifuged and cells were washed
421 with PBS, then resuspended. CV was added (final 0.01% w/v), vortexed and incubated for
422 10 minutes. Cells were washed 3 times, before being destained with 2 mL of 95% ethanol
423 for 10 minutes. Cell-free supernatant was then transferred into spectroscopic cuvettes and
424 absorbance is measured at 540 nm.

425

426 *Galleria mellonella* infection model. Larvae survival assay was performed as previously
427 described (53). Ten larvae per group.

428

429 Checkerboard Assay was performed as described previously: (54). 4 x10^4 bacteria, with

430 MOI: 5000, 500, 50, 5, 0.5, 0.05, 0.005.

431

References

1. Leptihn S. 2019. Welcome back to the Pre-Penicillin Era. Why we desperately need new strategies in the battle against bacterial pathogens. Infect Microbes Dis 1:33. https://doi.org/10.1097/IM9.0000000000000009.
2. Igler C, Rolff J, Regoes R. 2021. Multi-step vs. single-step resistance evolution under different drugs, pharmacokinetics, and treatment regimens. eLife 10:e64116. https://doi.org/10.7554/eLife.64116.
3. Holmes AH, Moore LS, Sundsfjord A, Steinbakk M, Regmi S, Karkey A, Guerin PJ, Piddock LJ. 2016. Understanding the mechanisms and drivers of antimicrobial resistance. The Lancet 387:176-187. https://doi.org/10.1016/S0140-6736(15)00473-0.
4. Loh B, Chen J, Manohar P, Yu Y, Hua X, Leptihn S. 2020. A Biological Inventory of Prophages in A. baumannii Genomes Reveal Distinct Distributions in Classes, Length, and Genomic Positions. Frontiers in microbiology 11. https://doi.org/10.3389/fmicb.2020.579802.
5. Lepore C, Silver L, Theuretzbacher U, Thomas J, Visi D. 2019. The small-molecule antibiotics pipeline: 2014-2018. Nature Reviews Drug Discovery 18:739-740. https://doi.org/10.1038/d41573-019-00130-8.
6. Loh B, Leptihn S. 2020. A Call For a Multidisciplinary Future of Phage Therapy to Combat Multi-drug Resistant Bacterial Infections. Infectious Microbes & Diseases 2:1-2. https://doi.org/10.1097/im9.0000000000000018.
7. Gordillo Altamirano Fernando L, Barr Jeremy J. 2019. Phage Therapy in the Post-antibiotic Era. Clinical Microbiology Reviews 32:e00066-18. https://doi.org/10.1128/CMR.00066-18.

8. Viertel TM, Ritter K, Horz H-P. 2014. Viruses versus bacteria—novel approaches to phage therapy as a tool against multidrug-resistant pathogens. Journal of Antimicrobial Chemotherapy 69:2326-2336. https://doi.org/10.1093/jac/dku173.

9. Kortright KE, Chan BK, Koff JL, Turner PE. 2019. Phage Therapy: A Renewed Approach to Combat Antibiotic-Resistant Bacteria. Cell Host & Microbe 25:219-232. https://doi.org/https://doi.org/10.1016/j.chom.2019.01.014.

10. Labrie SJ, Samson JE, Moineau S. 2010. Bacteriophage resistance mechanisms. Nature Reviews Microbiology 8:317-327. https://doi.org/10.1038/nrmicro2315.

11. Tkhilaishvili T, Winkler T, Müller M, Perka C, Trampuz A. 2019. Bacteriophages as Adjuvant to Antibiotics for the Treatment of Periprosthetic Joint Infection Caused by Multidrug-Resistant Pseudomonas aeruginosa. Antimicrobial agents and chemotherapy 64:e00924-19. https://doi.org/10.1128/AAC.00924-19.

12. Gordillo Altamirano FL, Barr JJ. 2021. Unlocking the next generation of phage therapy: the key is in the receptors. Current Opinion in Biotechnology 68:115-123. https://doi.org/https://doi.org/10.1016/j.copbio.2020.10.002.

13. Sun B, Liu H, Jiang Y, Shao L, Yang S, Chen D. 2020. New Mutations Involved in Colistin Resistance in Acinetobacter baumannii. mSphere 5:e00895-19. https://doi.org/10.1128/mSphere.00895-19.

14. Mu X, Wang N, Li X, Shi K, Zhou Z, Yu Y, Hua X. 2016. The effect of colistin resistance-associated mutations on the fitness of Acinetobacter baumannii. Frontiers in microbiology 7:1715. https://doi.org/10.3389/fmicb.2016.01715.

15. Arroyo LA, Herrera CM, Fernandez L, Hankins JV, Trent MS, Hancock REW. 2011. The pmrCAB operon mediates polymyxin resistance in Acinetobacter baumannii ATCC 17978 and clinical isolates through phosphoethanolamine modification of lipid A. Antimicrobial agents and chemotherapy 55:3743-3751. https://doi.org/10.1128/AAC.00256-11

16. Jayol A, Poirel L, Brink A, Villegas M-V, Yilmaz M, Nordmann P. 2014. Resistance to colistin associated with a single amino acid change in protein PmrB among Klebsiella pneumoniae isolates of worldwide origin. Antimicrobial agents and chemotherapy 58:4762-4766. https://doi.org/10.1128/AAC.00084-14

17. Phan M-D, Nhu NTK, Achard MES, Forde BM, Hong KW, Chong TM, Yin W-F, Chan K-G, West NP, Walker MJ, Paterson DL, Beatson SA, Schembri MA. 2017. Modifications in the pmrB gene are the primary mechanism for the development of chromosomally encoded resistance to polymyxins in uropathogenic Escherichia coli. Journal of Antimicrobial Chemotherapy 72:2729-2736. https://doi.org/10.1093/jac/dkx204.

18. Tynecki P, Guziński A, Kazimierczak J, Jadczuk M, Dastych J, Onisko A. 2020. PhageAI-Bacteriophage Life Cycle Recognition with Machine Learning and Natural Language Processing. BioRxiv doi:10.1101/2020.07.11.198606. https://doi.org/10.1101/2020.07.11.198606.

19. Wielgoss S, Bergmiller T, Bischofberger AM, Hall AR. 2016. Adaptation to Parasites and Costs of Parasite Resistance in Mutator and Nonmutator Bacteria. Molecular Biology and Evolution 33:770-782. https://doi.org/10.1093/molbev/msv270.

20. Deatherage DE, Barrick JE. 2014. Identification of mutations in laboratory-evolved microbes from next-generation sequencing data using breseq, p 165-188, Engineering and analyzing multicellular systems doi:10.1007/978-1-4939-0554-6_12. Springer.

21. Xu Q, Chen T, Yan B, Zhang L, Pi B, Yang Y, Zhang L, Zhou Z, Ji S, Leptihn S, Akova M, Yu Y, Hua X. 2019. Dual Role of gnaA in Antibiotic Resistance and Virulence in Acinetobacter baumannii. Antimicrobial agents and chemotherapy 63:e00694-19. https://doi.org/10.1128/AAC.00694-19.

507 22. Kuo S-C, Yang S-P, Lee Y-T, Chuang H-C, Chen C-P, Chang C-L, Chen T-L, Lu P-
508 L, Hsueh P-R, Fung C-P. 2013. Dissemination of imipenem-resistant Acinetobacter
509 baumannii with new plasmid-borne blaOXA-72 in Taiwan. BMC Infectious Diseases
510 13:319. https://doi.org/10.1186/1471-2334-13-319.
511 23. Pelletier MR, Casella LG, Jones JW, Adams MD, Zurawski DV, Hazlett KRO, Doi Y,
512 Ernst RK. 2013. Unique structural modifications are present in the lipopolysaccha-
513 ride from colistin-resistant strains of Acinetobacter baumannii. Antimicrobial agents
514 and chemotherapy 57:4831-4840. https://doi.org/10.1128/AAC.00865-13.
515 24. Talyansky Y, Nielsen TB, Yan J, Carlino-Macdonald U, Di Venanzio G, Chakravorty
516 S, Ulhaq A, Feldman MF, Russo TA, Vinogradov E, Luna B, Wright MS, Adams
517 MD, Spellberg B. 2021. Capsule carbohydrate structure determines virulence in
518 Acinetobacter baumannii. PLOS Pathogens 17:e1009291.
519 https://doi.org/10.1371/journal.ppat.1009291.
520 25. Harding CM, Hennon SW, Feldman MF. 2018. Uncovering the mechanisms of Aci-
521 netobacter baumannii virulence. Nature Reviews Microbiology 16:91-102.
522 https://doi.org/10.1038/nrmicro.2017.148.
523 26. Weber Brent S, Harding Christian M, Feldman Mario F, Margolin W. 2016. Patho-
524 genic Acinetobacter: from the Cell Surface to Infinity and Beyond. Journal of Bacte-
525 riology 198:880-887. https://doi.org/10.1128/JB.00906-15.
526 27. Hua X, Liang Q, Fang L, He J, Wang M, Hong W, Leptihn S, Wang H, Yu Y, Chen
527 H. 2020. Bautype: Capsule and Lipopolysaccharide Serotype Prediction for Aci-
528 netobacter baumannii Genome. Infectious Microbes & Diseases 2.
529 https://doi.org/10.1097/IM9.0000000000000019.
530 28. Gu Liu C, Green SI, Min L, Clark JR, Salazar KC, Terwilliger AL, Kaplan HB, Tra-
531 utner BW, Ramig RF, Maresso AW. 2020. Phage-Antibiotic Synergy Is Driven by a

532 Unique Combination of Antibacterial Mechanism of Action and Stoichiometry. mBio
533 11:e01462-20. https://doi.org/10.1128/mBio.01462-20.
534 29. Ryan EM, Alkawareek MY, Donnelly RF, Gilmore BF. 2012. Synergistic phage-
535 antibiotic combinations for the control of Escherichia coli biofilms in vitro. FEMS
536 Immunology & Medical Microbiology 65:395-398. https://doi.org/10.1111/j.1574-
537 695X.2012.00977.x.
538 30. Sørensen MCH, van Alphen LB, Harboe A, Li J, Christensen BB, Szymanski CM,
539 Brøndsted L. 2011. Bacteriophage F336 recognizes the capsular phosphoramidate
540 modification of Campylobacter jejuni NCTC11168. Journal of bacteriology
541 193:6742-6749. https://doi.org/10.1128/JB.05276-11.
542 31. Knirel YA, Shneider MM, Popova AV, Kasimova AA, Senchenkova SN, Shashkov
543 AS, Chizhov AO. 2020. Mechanisms of Acinetobacter baumannii Capsular Polysac-
544 charide Cleavage by Phage Depolymerases. Biochemistry (Moscow) 85:567-574.
545 https://doi.org/10.1134/S0006297920050053.
546 32. Liu Y, Mi Z, Mi L, Huang Y, Li P, Liu H, Yuan X, Niu W, Jiang N, Bai C, Gao Z.
547 2019. Identification and characterization of capsule depolymerase Dpo48 from Aci-
548 netobacter baumannii phage IME200. PeerJ 7:e6173.
549 https://doi.org/10.7717/peerj.6173.
550 33. Oliveira H, Costa AR, Konstantinides N, Ferreira A, Akturk E, Sillankorva S, Nemec
551 A, Shneider M, Dötsch A, Azeredo J. 2017. Ability of phages to infect Acinetobacter
552 calcoaceticus□Acinetobacter baumannii complex species through acquisition of dif-
553 ferent pectate lyase depolymerase domains. Environmental microbiology 19:5060-
554 5077. https://doi.org/10.1111/1462-2920.13970.
555 34. Gordillo Altamirano F, Forsyth JH, Patwa R, Kostoulias X, Trim M, Subedi D, Archer
556 SK, Morris FC, Oliveira C, Kielty L, Korneev D, O'Bryan MK, Lithgow TJ, Peleg AY,
557 Barr JJ. 2021. Bacteriophage-resistant Acinetobacter baumannii are resensitized to

558 antimicrobials. Nature Microbiology 6:157-161. https://doi.org/10.1038/s41564-020-
559 00830-7.
560 35. Hesse S, Rajaure M, Wall E, Johnson J, Bliskovsky V, Gottesman S, Adhya S, Hat-
561 full Graham F. 2020. Phage Resistance in Multidrug-Resistant Klebsiella pneu-
562 moniae ST258 Evolves via Diverse Mutations That Culminate in Impaired Adsorp-
563 tion. mBio 11:e02530-19. https://doi.org/10.1128/mBio.02530-19.
564 36. Filippov AA, Sergueev KV, He Y, Huang X-Z, Gnade BT, Mueller AJ, Fernandez-
565 Prada CM, Nikolich MP. 2011. Bacteriophage-resistant mutants in Yersinia pestis:
566 identification of phage receptors and attenuation for mice. PloS one 6:e25486.
567 https://doi.org/10.1371/journal.pone.0025486.
568 37. Cai R, Wang G, Le S, Wu M, Cheng M, Guo Z, Ji Y, Xi H, Zhao C, Wang X. 2019.
569 Three capsular polysaccharide synthesis-related glucosyltransferases, GT-1, GT-2
570 and WcaJ, are associated with virulence and phage sensitivity of Klebsiella pneu-
571 moniae. Frontiers in microbiology 10:1189.
572 https://doi.org/10.3389/fmicb.2019.01189.
573 38. Oechslin F. 2018. Resistance development to bacteriophages occurring during bac-
574 teriophage therapy. Viruses 10:351. https://doi.org/10.3390/v10070351.
575 39. León M, Bastías R. 2015. Virulence reduction in bacteriophage resistant bacteria.
576 Frontiers in microbiology 6:343. https://doi.org/10.3389/fmicb.2015.00343.
577 40. Burmeister AR, Turner PE. 2020. Trading-off and trading-up in the world of bacte-
578 ria–phage evolution. Current Biology 30:R1120-R1124.
579 https://doi.org/https://doi.org/10.1016/j.cub.2020.07.036.
580 41. Aslam S, Courtwright AM, Koval C, Lehman SM, Morales S, Furr CLL, Rosas F,
581 Brownstein MJ, Fackler JR, Sisson BM. 2019. Early clinical experience of bacterio-
582 phage therapy in 3 lung transplant recipients. American Journal of Transplantation
583 19:2631-2639. https://doi.org/10.1111/ajt.15503

584 42. Johnson JK, Robinson GL, Pineles LL, Ajao AO, Zhao L, Albrecht JS, Harris AD,
585 Thom KA, Furuno JP. 2017. Carbapenem MICs in Escherichia coli and Klebsiella
586 Species Producing Extended-Spectrum β-Lactamases in Critical Care Patients from
587 2001 to 2009. Antimicrobial agents and chemotherapy 61:e01718-16.
588 https://doi.org/10.1128/AAC.01718-16.
589 43. Tagliaferri TL, Jansen M, Horz H-P. 2019. Fighting pathogenic bacteria on two
590 fronts: phages and antibiotics as combined strategy. Frontiers in cellular and infec-
591 tion microbiology 9:22. https://doi.org/10.3389/fcimb.2019.00022.
592 44. Mangalea MR, Duerkop BA. 2020. Fitness Trade-Offs Resulting from Bacterio-
593 phage Resistance Potentiate Synergistic Antibacterial Strategies. Infection and im-
594 munity 88:e00926-19. https://doi.org/10.1128/IAI.00926-19.
595 45. Burmeister AR, Fortier A, Roush C, Lessing AJ, Bender RG, Barahman R, Grant R,
596 Chan BK, Turner PE. 2020. Pleiotropy complicates a trade-off between phage re-
597 sistance and antibiotic resistance. Proceedings of the National Academy of Scienc-
598 es 117:11207. https://doi.org/10.1073/pnas.1919888117
599 46. Wick RR, Judd LM, Gorrie CL, Holt KE. 2017. Unicycler: Resolving bacterial ge-
600 nome assemblies from short and long sequencing reads. PLOS Computational Bi-
601 ology 13:e1005595. https://doi.org/10.1371/journal.pcbi.1005595
602 47. Xu Q, Chen T, Yan B, Zhang L, Pi B, Yang Y, Zhang L, Zhou Z, Ji S, Leptihn S,
603 Akova M, Yu Y, Hua X. Dual Role of gnaA in Antibiotic Resistance and Virulence in
604 Acinetobacter baumannii. Antimicrobial Agents and Chemotherapy 63:e00694-19.
605 https://doi.org/10.1128/AAC.00694-19
606 48. Shi Y, Hua X, Xu Q, Yang Y, Zhang L, He J, Mu X, Hu L, Leptihn S, Yu Y. 2020.
607 Mechanism of eravacycline resistance in Acinetobacter baumannii mediated by a
608 deletion mutation in the sensor kinase adeS, leading to elevated expression of the

efflux pump AdeABC. Infection, Genetics and Evolution 80:104185. https://doi.org/https://doi.org/10.1016/j.meegid.2020.104185

49. Leptihn S, Har JY, Chen J, Ho B, Wohland T, Ding JL. 2009. Single molecule resolution of the antimicrobial action of quantum dot-labeled sushi peptide on live bacteria. BMC Biology 7:22. https://doi.org/10.1186/1741-7007-7-22

50. Caroff M, Novikov A. 2020. Lipopolysaccharides: structure, function and bacterial identifications. OCL (Oilseeds, Crops, fats & Lipids) 27:31. https://doi.org/https://doi.org/10.1051/ocl/2020025.

51. Davis Jr MR, Goldberg JB. May 2012. Purification and visualization of lipopolysaccharide from Gram-negative bacteria by hot aqueousphenol extraction. J Vis Exp 28 http://dx doi org/103791/3916.

52. Hu L, Shi Y, Xu Q, Zhang L, He J, Jiang Y, Liu L, Leptihn S, Yu Y, Hua X, Zhou Z. 2020. Capsule Thickness, Not Biofilm Formation, Gives Rise to Mucoid Acinetobacter baumannii Phenotypes That are More Prevalent in Long-Term Infections: A Study of Clinical Isolates from a Hospital in China. Infection and drug resistance 13:99-109. https://doi.org/10.2147/IDR.S230178.

53. Richmond Grace E, Evans Laura P, Anderson Michele J, Wand Matthew E, Bonney Laura C, Ivens A, Chua Kim L, Webber Mark A, Sutton JM, Peterson Marnie L, Piddock Laura JV, Wright Gerard D, Schafer W, Hancock R. The Acinetobacter baumannii Two-Component System AdeRS Regulates Genes Required for Multidrug Efflux, Biofilm Formation, and Virulence in a Strain-Specific Manner. mBio 7:e00430-16. https://doi.org/10.1128/mBio.00430-16.

54. Gu Liu C, Green Sabrina I, Min L, Clark Justin R, Salazar Keiko C, Terwilliger Austen L, Kaplan Heidi B, Trautner Barbara W, Ramig Robert F, Maresso Anthony W, Sperandio V. Phage-Antibiotic Synergy Is Driven by a Unique Combination of Anti-

634 bacterial Mechanism of Action and Stoichiometry. mBio 11:e01462-20.
635 https://doi.org/10.1128/mBio.01462-20.

Figure legends

Figure 1: Phage Phab24 and effect on *A. baumannii* strain growth dynamics. (A) Transmission electron micrograph of Phab24 (negative staining). Phage Phab24 belongs to Myoviridae which have contractible tails (as seen on the right). Bar: 200nm. (B) Growth curves of the *A. baumannii* reference strain ATCC17978 and phage-resistant reconstructed strains with introduced genomic mutations in the putative amylovoran biosynthesis gene *amsE* or in the putative LPS biogenesis gene ("*lpsBSP*"), and their plasmid-complementations (::*asmE* and ::*lpsBSP*) in the presence or absence of phage Phab24. (C) Spot testing of Phab24 on agar containing phage-resistant and susceptible strains.

Figure 2: Attachment assay of Phab24 to bacteria. Titre of free phages detected in media after incubation with (A) reference strain ATCC17978, colistin resistant derivate XH198 as well as the *amsE* and *lpsBSP* genetically engineered strains (Δ) and their complementations (::), and (B) Phab24 phage-resistant colonies, "R", derived from ATCC17978. Control: phage Phab24 incubated without bacteria. XH194: bacterial strain that is colistin resistant and is not infected by Phab24.

Figure 3: Composition of the bacterial envelope.

(A to C) Mass spectrometry (positive mode) analysis of lipid A isolated using aqueous phenol extraction from (A) Wildtype strain ATCC17978, (B) Phab24 resistant, genetically introduced reconstructed *lpsBSP* gene mutant on ATCC17978, (C) Plasmid complemented Phab24 resistant strain. (D&E) SDS-PAGE gel of isolated capsular polysaccharides stained with (D) Alcian blue, which allows the detection of acidic polysaccharides, and (E) silver staining, which detects lipids and proteins/peptides.

Figure 4: Surface structure of bacterial cell envelope. Scanning Electron Microscopy. Δ*lpsBSP*: knock-out of *lpsBSP* gene in the ATCC17978. Δ*lpsBSP::lpsBSP*: knock-out of *lpsBSP* gene which was complemented with the wildtype *lpsBSP* gene *in trans*. Δ*amsE*: knock-out of *amsE* gene in the ATCC17978. Δ*amsE::amsE*: knock-out of *amsE* gene which was complemented with the wildtype *amsE* gene *in trans*.

Figure 5: Biofilm formation and capsular stain. (A) Biofilm formation assessed by the ability to retain crystal violet (CV) dye. Strains were incubated for 72 hours in multi well plates without shaking. (B) Capsule stain of planktonic cells incubated for 8 hours with shaking. Cells were stained with CV to determine the ability of the bacterial capsule to retain the dye. Ethanol was used to destain the capsule and release the CV dye which was then detected by measuring absorbance at 540nm.

Figure 6: *In vivo* virulence tests of *A. baumannii* strains and the Phab24 resistant isolates. Survival of *Galleria melonella* larvae over 120 h after injection with (A) 10^6 colony forming units (CFU), (B) 10^7 CFU, and (C) 10^8 CFU of *A. baumannii* strains. Each group consisted of 10 larvae. Shown is a representative experiment of 4 independent repeats.

Figure 7: Colistin and Phage resistance. (A) Synergy of colistin with/without phage Phab24. Co-incubation of different numbers of Phab24 (MOI) at different concentrations of colistin (mg/L) at constant cell numbers. Each circle represents an independent experiment. (B&C) Colistin-resistance levels of emerged phage-resistant colonies. Colony count of XH198 incubated for 3 h in the absence of colistin or on colistin plates with different antibiotic concentrations (B) in the absence of phage, and (C) in the presence of Phab24. (D) Colistin MIC of selected Phab24 resistant isolates. Top panel shows if the

strain can be infected by Phab24, indicating successful complementation of a mutated gene. The control, strain XH198, exhibits a MIC of 64 mg/L. Phage-resistant isolates displayed reduced levels of resistance varying from 16 - 1 mg/L, except for one strain (R81). The reconstructed *amsE* mutant shows an increased sensitivity to colistin compared to the reference strain XH198, while plasmid complementation with the wildtype gene fully restores the high level of resistance. The genetic deletion of the entire *lpsBSP* gene in XH198 appears does not result in a reduction in colistin resistance. However, strains with mutations that lead to a truncated *lpsBSP* gene product increase colistin sensitivity by 32-fold (R518, R587).

Table 1: Resistant strains and mutations conveying phage resistance and outcome of wildtype gene complementations *in trans*. Mutations were either detected by whole genome sequencing (strains R5, R10, R22, R23, R39, R70, R81, R83, R86, R115, R125, R130, R132, R134, R137), or screened for using mutation-specific primers.

Supplemental Materials

Supplemental Figure 1,2,3: Composition of the bacterial envelope. (1) Mass spectra with m/z values from 180 to 750 of polysaccharides isolated from the wildtype strain ATCC17978, or the Phab24 resistant, genetically engineered (reconstructed) *amsE* gene mutant on ATCC17978. (2) Mass spectra with m/z values from 750 to 1500 of polysaccharides isolated from the wildtype strain ATCC17978, or the Phab24 resistant, genetically engineered (reconstructed) *amsE* gene mutant on ATCC17978. (3) Mass spectra with m/z values from 1500 to 2300 of polysaccharides isolated from the wildtype strain ATCC17978, or the Phab24 resistant, genetically engineered (reconstructed) *amsE* gene mutant on ATCC17978.

Supplemental Figure 4: Surface structure of bacterial cell envelope. Thin sections of bacterial cells visualised by TEM. Two pictures representative of cells were chosen for each cell type. Δ*amsE*: knock-out of *amsE* gene in the ATCC reference strain. Δ*lpsBSP:* knock-out of *lpsBSP* gene in the ATCC reference strain.

Supplemental Figure 5: Membraneous structures and cell aggregation observed during experimental protocols using the ATCC17978 *amsE* KO mutant: (Top) Biofilm Assay (Bottom) Capsular staining.

Supplemental Table 1: A selection of Phage-resistant isolates with gene mutations that are not responsible for phage resistance. The mutations conveying resistance are indicated (unless unknown). Last column (right): Negative outcome of wildtype gene complementations in trans indicate that resistance is not mediated by these genes. Mutations were either detected by whole genome sequencing and confirmed by PCR (strains R5, R10, R22, R23, R39, R70, R81, R83, R86, R115, R125, R130, R132, R134, R137), or screened for using gene-specific primers.

Supplemental Table 2: Colistin MIC values of phage resistant isolates (individual strains) derived from XH198 determined by micro broth dilution method.

Figure 1

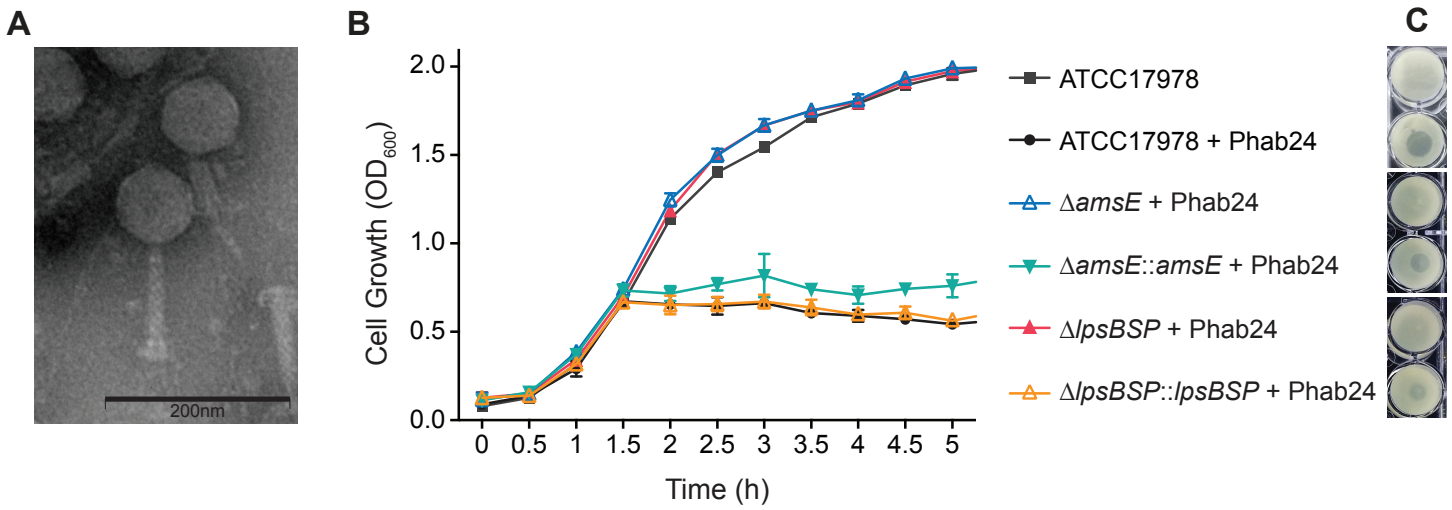

Figure 2

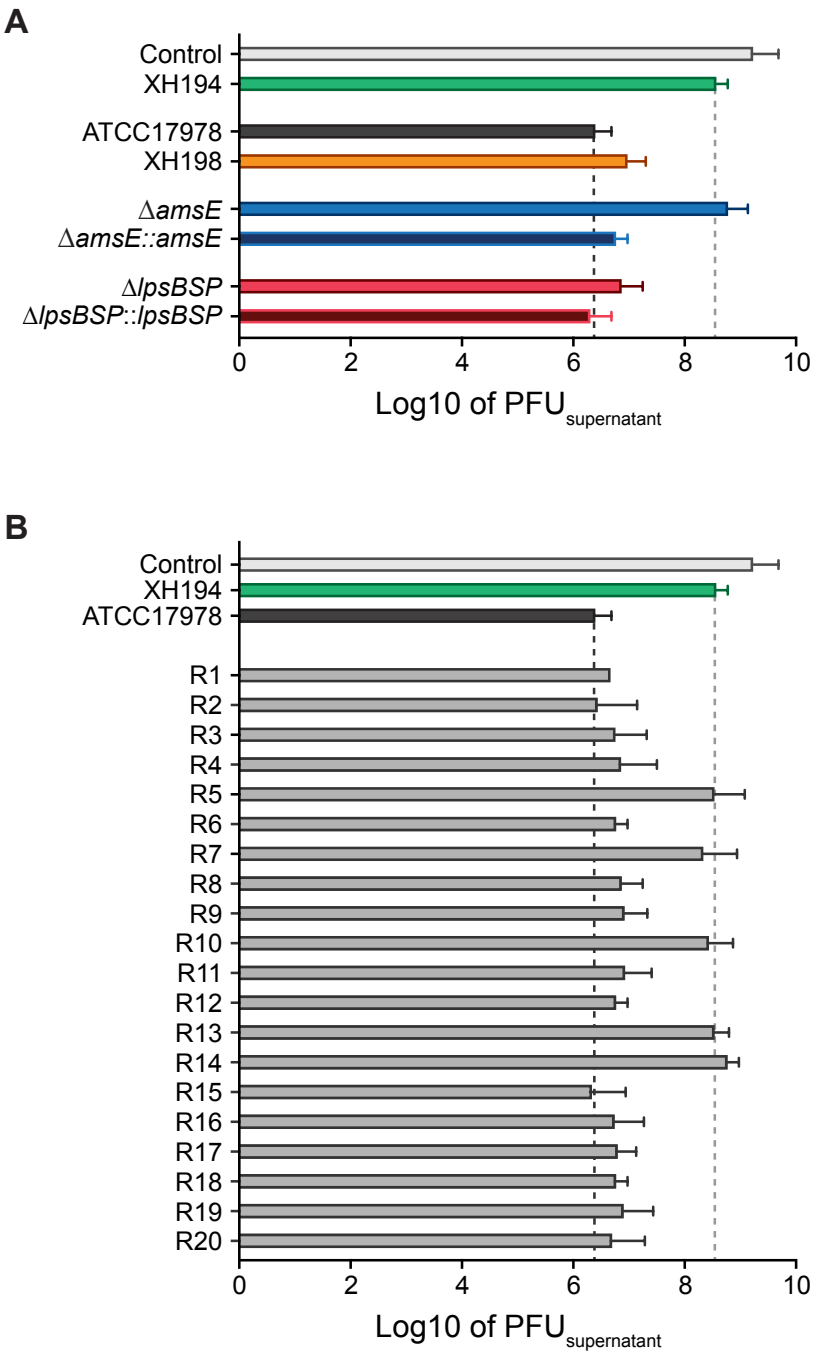

Figure 3

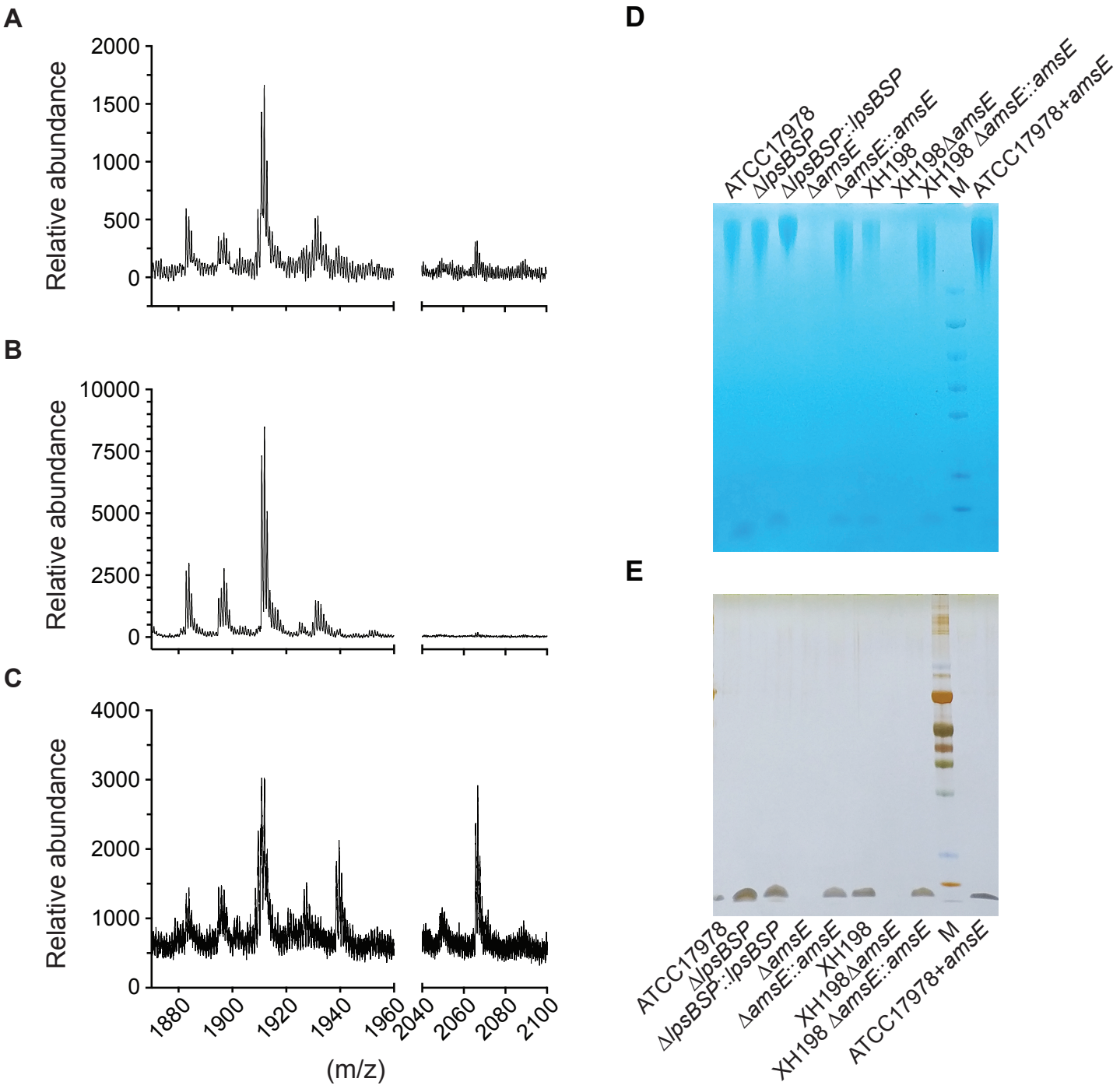

Figure 4

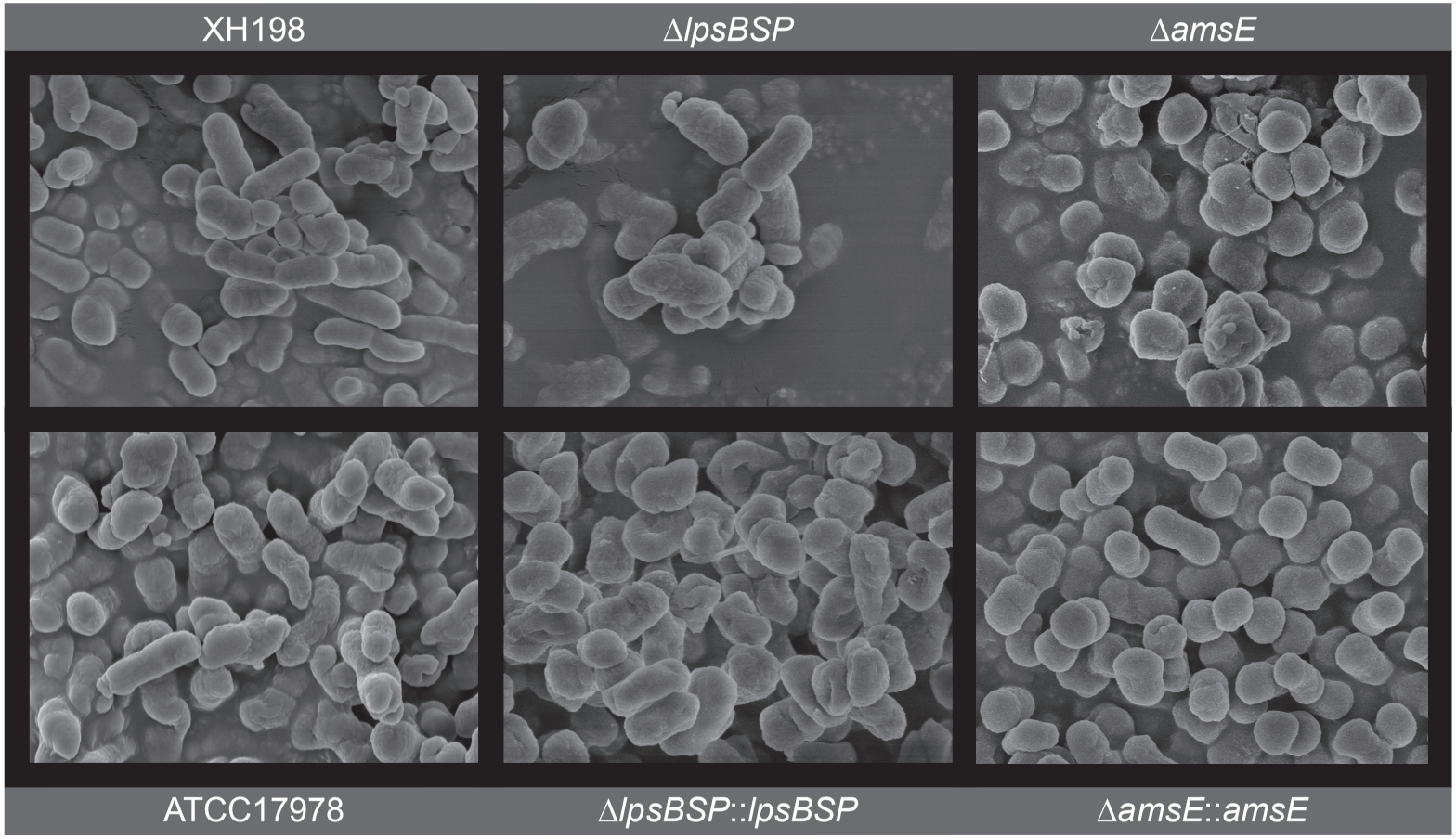

Figure 5

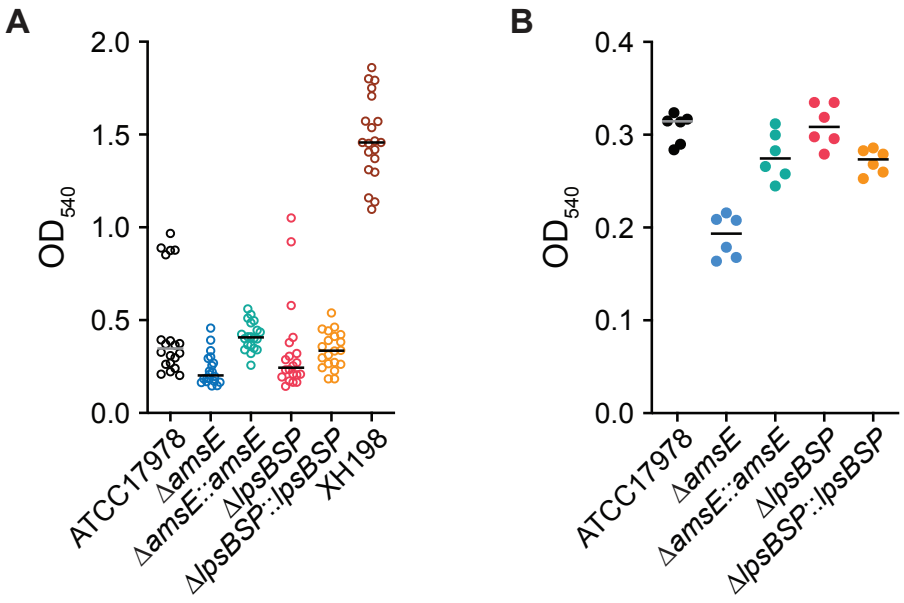

Figure 6

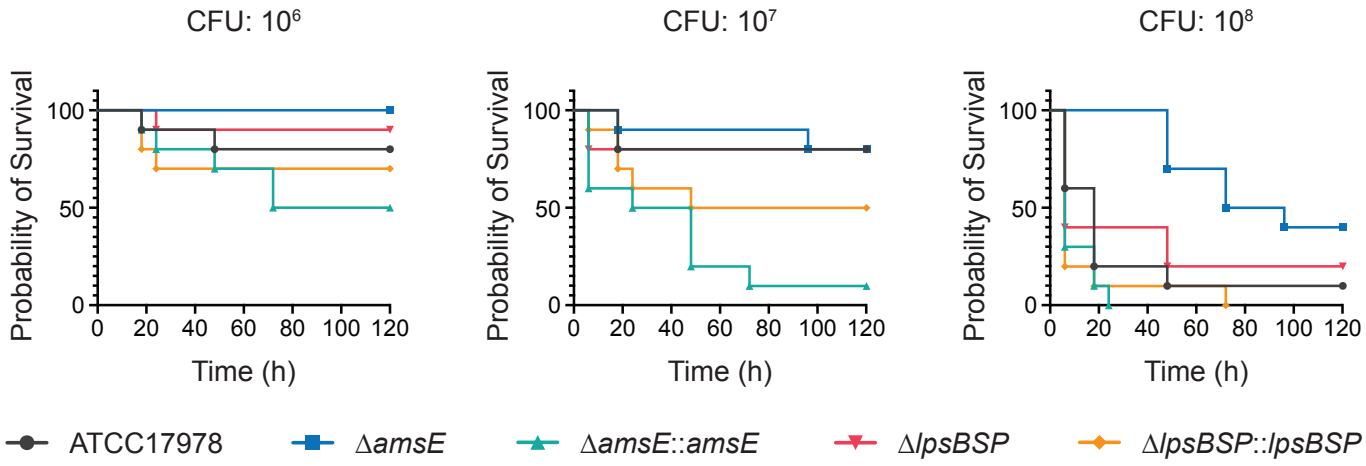

Figure 7

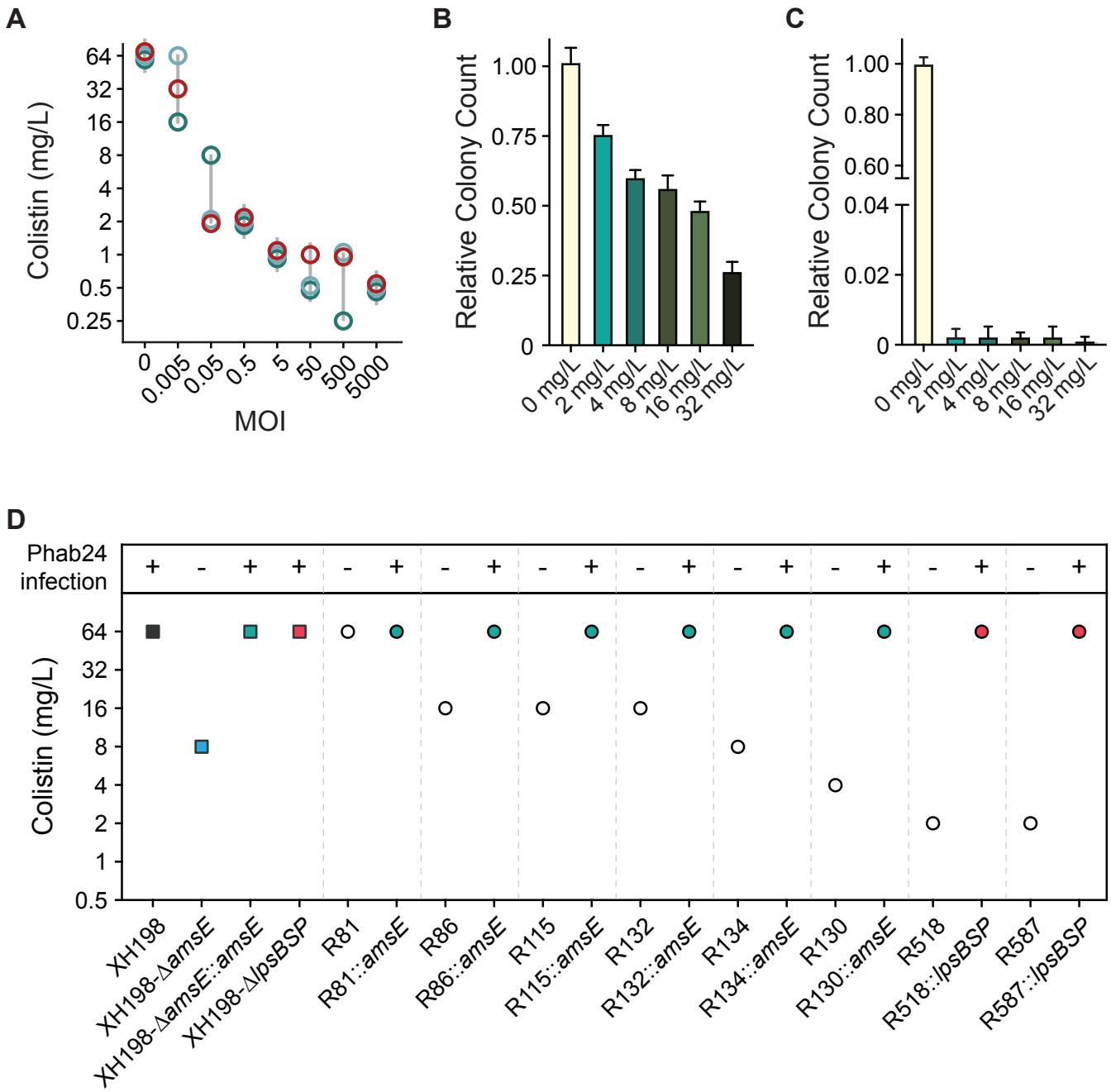

TABLE 1 Identified mutations in genes responsible for phage resistance and complementation results.

A selection of phage Phab24 resistant strains and mutations conveying resistance, and outcome of wildtype gene complementations *in trans*. Mutations were either detected by whole genome sequencing and confirmed by PCR (strains R5, R10, R22, R23, R39, R70, R81, R83, R86, R115, R125, R130, R132, R134, R137), or screened for using gene-specific primers.

			Complementation	
Resistant Isolate	**Mutation**	**Putative gene function**	**Yes**	**No**
R1	*lpsBSP* (IS4 family insertion)	LPS/ LOS biosynthesis	*lpsBSP*	
R2	*lpsBSP* (535th A loss, p.Asn179Ile fs Ter7)	LPS/ LOS biosynthesis	*lpsBSP*	
R5	amsE (IS4 insertion)	Amylovoran biosynthesis		*amsE*
	lpsBSP (535th A loss, p.Asn179Ile fs Ter7)	LPS/ LOS biosynthesis		*lpsBSP*
R7	*amsE* (IS5 insertion)	Amylovoran biosynthesis	*amsE*	
R8	*lpsBSP* (535th A loss, p.Asn179Ile fs Ter7)	LPS/ LOS biosynthesis	*lpsBSP*	
R10	*amsE* (559th T loss, p. Leu187Tyr fs Ter3)	Amylovoran biosynthesis	*amsE*	
R12	*lpsBSP* (535th A loss, p.Asn179Ile fs Ter7)	LPS/ LOS biosynthesis	*lpsBSP*	
R13	No PCR product of *amsE*	Amylovoran biosynthesis		*amsE*
R28	*amsE* (transposase insertion)	Amylovoran biosynthesis		*amsE*
R33	*amsE* (IS5 insertion)	Amylovoran biosynthesis		*amsE*
R35	*lpsBSP* (535th A loss, p.Asn179Ile fs Ter7)	LPS/ LOS biosynthesis	*lpsBSP*	
R39	*lpsBSP* (535th A loss, p.Asn179Ile fs Ter7)	LPS/ LOS biosynthesis	*lpsBSP*	
R54	*amsE* (transposase insertion)	Amylovoran biosynthesis		*amsE*
R78	*lpsBSP* (IS5 family insertion)	LPS/ LOS biosynthesis	*lpsBSP*	

Resistant Isolate	Mutation	Putative gene function	Complementation	
			Yes	No
amsE KO	Markerless knock out the entire *amsE* on the background of ATCC17978	Amylovoran biosynthesis	*amsE*	
lpsBSP-delta A	Subsititute for the wild type *lpsBSP* on the background of ATCC17978	LPS/ LOS biosynthesis	*lpsBSP*	
R81	*amsE* (transposase insertion)	Amylovoran biosynthesis	*amsE*	
R83	No PCR product of *amsE*	Amylovoran biosynthesis		*amsE*
R86	*amsE* (transposase insertion)	Amylovoran biosynthesis	*amsE*	
R115	*amsE* (transposase insertion)	Amylovoran biosynthesis	*amsE*	
R130	*amsE* (transposase insertion)	Amylovoran biosynthesis	*amsE*	
R132	*amsE* (transposase insertion)	Amylovoran biosynthesis		*amsE*
R134	*amsE* (transposase insertion)	Amylovoran biosynthesis	*amsE*	
XH198 *amsE* KO	Markerless knock out the entire *amsE* on the background of XH198	Amylovoran biosynthesis	*amsE*	
XH198 *lpsBSP*-KO	Markerless knock out the entire *lpsBSP* on the background of XH198	LPS/ LOS biosynthesis	*lpsBSP*	
R518	*lpsBSP* (535th A loss, p.Asn179Ile fs Ter7)	LPS/ LOS biosynthesis	*lpsBSP*	
R587	*lpsBSP* (535th A loss, p.Asn179Ile fs Ter7)	LPS/ LOS biosynthesis	*lpsBSP*	

Yes: After the transformation of the corresponding plasmid which contains the WT gene, the R variant can get infected by Phab24.

No: After the transformation of the corresponding plasmid which contains the WT gene, the R variant cannot get infected by Phab24.

R1-R80 are Phab24 escape mutants from ATCC17978.
R81-R587 are Phab24 escape variants from XH198.
Based on the NCBI accession number CP018664.1, ATCC17978:

AUO97-06900, *amsE*, 828nt

AUO97-03485, *lpsBSP*, 768nt